NPPS-2008, Moscow, Russia, July, 7–10, 2008

APPLYING L. MANEVITCH'S COMPLEXIFICATION – AVERAGING METHOD TO ANALYZE CONDITIONS FOR OPTIMAL TARGETED ENERGY TRANSFER IN COUPLED OSCILLATORS WITH ESSENTIAL STIFFNESS NONLINEARITY

Themistoklis Sapsis [a], D. Dane Quinn [b], Oleg Gendelman [c], Alexander Vakakis [d,e], Lawrence Bergman [f], Gaetan Kerschen [g]

[a] *Department of Mechanical Engineering, Massachusetts Institute of Technology, USA*

[b] *Department of Mechanical Engineering, The University of Akron, USA*

[c] *Faculty of Mechanical Engineering, Technion—Israel Institute of Technology, Israel*

[d] *Division of Mechanics, National Technical University of Athens, Greece*

[e] *Department of Mechanical Science and Engineering (Adjunct), University of Illinois at Urbana-Champaign, USA*

[f] *Department of Aerospace Engineering, University of Illinois at Urbana-Champaign, USA*

[g] *Aerospace and Mechanical Engineering Department (LTAS), Université de Liège, Belgium*

Abstract

We study targeted energy transfer (TET) [1] from a linear damped oscillator (LO) to a light attachment with essential stiffness nonlinearity, caused by 1:1 transient resonance capture (TRC). First, we study the underlying Hamiltonian dynamics and show that for sufficiently weak damping, the nonlinear damped transitions of the system are strongly influenced by the underlying topological structure of periodic and quasiperiodic orbits of the hamiltonian system. Then, we formulate conditions that lead to effective or even optimal TET from the linear system to the nonlinear attachment. Direct analytical treatment of the governing strongly nonlinear damped equations of motion is performed by applying L. Manevitch's complexification – averaging (CX-A) method [2] to perform slow-fast partition of the transient responses, and analytically model the dynamics in the region of optimal TET. This analysis determines the characteristic time scales of the dynamics that influence the capacity of the nonlinear attachment to passively absorb and locally dissipate broadband energy from the linear oscillator in an optimal fashion.

Key words: Bifurcations, Modeling

1. Introduction

The aim of this work is to study the complex transitions in the dynamics and targeted energy transfers associated with the attraction of the transient dynamics of a two DOF strongly nonlinear system into 1:1 resonance capture [Arnold et al.]. In particular, we consider the following weakly damped system

$$\begin{aligned} &\ddot{x} + \lambda_1 \dot{x} + \lambda_2 (\dot{x} - \dot{v}) + \omega_0^2 x + C(x - v)^3 = 0 \\ &\varepsilon \ddot{v} + \lambda_2 (\dot{v} - \dot{x}) + C(v - x)^3 = 0 \end{aligned} \qquad (1)$$

viewed as a linear oscillator (LO), described by *x*, coupled to a nonlinear energy sink (NES) whose response is measured by *v*.

As reported in earlier works [Kerschen et al.] the two DOF system under consideration possesses surprisingly complex dynamics. Moreover, at certain ranges of parameters and initial conditions passive targeted energy transfer—TET—is possible, whereby vibration energy initially localized in the linear oscillator gets passively transferred to the lightweight attachment in a one-way irreversible fashion.

The first section of this work deals with the underlying structure of the Hamiltonian dynamics of the system. Then, a detailed computational study of the different types of nonlinear transitions that occur in the weakly damped system is presented. In the third section direct analytical treatment of the governing strongly nonlinear equations of motions is performed in order to analytically model the dynamics the region of optimal TET.

2. Topological features of the Hamiltonian dynamics

We consider system (1) with $\lambda_1 = \lambda_2 = 0$ and without loss of generality we set $\omega_0 = 1$,

$$\begin{aligned} &\ddot{x} + x + C(x - v)^3 = 0 \\ &\varepsilon \ddot{v} + C(v - x)^3 = 0 \end{aligned} \qquad (2)$$

We assume the following *ansatz* for the solution,

$$x(t) \approx \frac{a_1(t)}{\omega} \cos\left[\omega t + \alpha(t)\right],\ v(t) \approx \frac{a_2(t)}{\omega} \cos\left[\omega t + \beta(t)\right] \qquad (3)$$

Additionally, by introducing the phase difference angle $\phi = \alpha - \beta$, we obtain the following three-dimensional autonomous dynamical system on the cylinder $(R^2 \times S^1)$, that govern the slow evolution of the amplitudes $a_1(t),\ a_2(t)$ and the phase difference ϕ of the two oscillators.

$$\begin{aligned} \dot{a}_1 &= \frac{-3a_2 C}{8} \sin\phi \left[\left(a_1^2 + a_2^2\right) - 2a_1 a_2 \cos\phi\right] \\ \dot{a}_2 &= \frac{3a_1 C}{8\varepsilon} \sin\phi \left[\left(a_1^2 + a_2^2\right) - 2a_1 a_2 \cos\phi\right] \end{aligned} \qquad (4)$$

$$\dot{\phi} = \frac{1}{2} - \frac{3C}{8}\left[\left(a_1^2 + a_2^2\right) - 2a_1 a_2 \cos\phi\right]\left[\left(\frac{1}{\varepsilon}\right)\left[1 - \frac{a_1}{a_2}\cos\phi\right] - \left[1 - \frac{a_2}{a_1}\cos\phi\right]\right]$$

Note that the *ansatz* (3) indicates that conditions of 1:1 internal resonance are realized in the dynamics, so that the harmonic components at frequency ω dominate over all other higher harmonics.

It turns out that the dynamical system (4) is fully integrable, as there exist two first integrals of motion:

$$a_1^2 + \left(\sqrt{\varepsilon} a_2\right)^2 \equiv r^2 \quad \text{and} \quad \frac{a_1^2}{2} + \varepsilon\frac{a_2^2}{4} + \frac{3C}{32}\left(a_1^2 + a_2^2 - 2a_1 a_2 \cos\phi\right)^2 \equiv h \tag{5}$$

The first equation (energy conservation) enables us to introduce a second angle ψ into the problem,

$$\tan\left(\frac{\psi}{2} + \frac{\pi}{4}\right) = \frac{a_1}{\sqrt{\varepsilon a_2}}, \quad \psi \in \left[-\frac{\pi}{2}, \frac{\pi}{2}\right] \tag{6}$$

Taking into account the first integrals (5) and introducing the new angle into the problem, the slow-flow dynamical system (4) can be further reduced to

$$\begin{aligned}
&\dot{r} = 0 \\
&\dot{\psi} = \frac{-3Cr^2}{8\varepsilon^{3/2}}\left[(1+\varepsilon) - (1-\varepsilon)\sin\psi - 2\sqrt{\varepsilon}\cos\psi\cos\phi\right]\sin\phi \\
&\dot{\phi} = \frac{1}{2} - \frac{3Cr^2}{16\varepsilon^2}\left[1 + \varepsilon - (1-\varepsilon)\sin\psi - 2\sqrt{\varepsilon}\cos\psi\cos\phi\right]\left[1 - \varepsilon - 2\varepsilon^{1/2}\frac{\sin\psi\cos\phi}{\cos\psi}\right]
\end{aligned} \tag{7}$$

where $(r, \phi, \psi) \in (R^+ \times S^1 \times S^1)$. The additional first integral of the motion can be expressed in the form,

$$\frac{r^2}{8}\left(3 + \sin\psi + \frac{3Cr^2}{16\varepsilon^2}\left[(1+\varepsilon) - (1-\varepsilon)\sin\psi - 2\varepsilon^{1/2}\cos\psi\cos\phi\right]^2\right) = h \tag{8}$$

Considering the isoenergetic dynamical flow for $r = const$, the orbits of the system lie an a topological 2-sphere, and follow the level sets of the first integral of motion (8).

Projections of the isoenergetic reduced dynamics unto the unit disk at different energy levels are shown in Figure 1. The north pole (NP) at

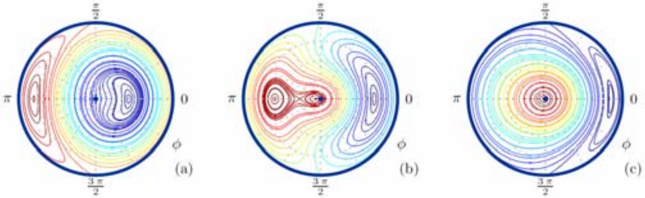

Figure 1. Projection of the dynamics of the isoenergetic manifold onto the unit disk at different energy levels (ε =0.1, C=2/15) (a) r = 1.00, (b) r = 0.375, (c) r = 0.25.

$\psi = \pi/2$ lies at the center of the disk, while the south pole (SP) $\psi = -\pi/2$ is mapped onto the entire unit circle. In this projection, trajectories that pass through the SP approach the unit circle at $\phi = \pi/2$ and are continued at $\phi = -\pi/2$. If the response is localized to the LO, so that $a_2 << a_1$, the phase variable ψ lies close to $+\pi/2$. In contrast, a localized response in the nonlinear attachment (e.g, $a_1 << a_2$) implies that $\psi \approx -\pi/2$.

Equilibrium points of the slow-flow (7) are explicitly evaluated by following expressions,

$$\dot{\psi} = 0 \Rightarrow \sin\phi_{\mathrm{eq}} = 0 \Rightarrow \ \phi_{\mathrm{eq}} = 0, \pi$$

$$\dot{\phi} = 0 \ \Rightarrow \cos\psi_{\mathrm{eq}} = \frac{3Cr^2}{8\varepsilon}(1+\varepsilon)^2\left[1 - \sin(\psi_{\mathrm{eq}} + \gamma_{\mathrm{eq}})\right]\cos(\psi_{\mathrm{eq}} + \gamma_{\mathrm{eq}})$$

with $\tan\gamma_{\mathrm{eq}} = 2\sqrt{\varepsilon}\cos\phi_{\mathrm{eq}} \Big/ (1-\varepsilon)$.

In general, equilibrium points for which $\phi_{\mathrm{eq}} = 0$ correspond to an in-phase motion and have been denoted as S11+ by [Kerschen et al.]. Those corresponding to $\phi_{\mathrm{eq}} = \pi$, represent out-of-phase periodic motions and have been denoted as $S11-$. In the projections of phase space shown in Figure 1, periodic motions on $S11+$ appear as equilibrium points that lie on the horizontal axis to the right of the origin, whereas periodic motions on $S11-$ as equilibrium points that lie on the horizontal axis to the left of the origin.

With increasing energy, e.g., as $r \rightarrow \infty$, both equilibrium points approach the value,

$$\lim_{r\to\infty} \psi_{\mathrm{eq}} = \arctan\left((1-\varepsilon)\Big/ 2\sqrt{\varepsilon}\cos\phi_{\mathrm{eq}}\right) \qquad (9)$$

so that, for $0 < \varepsilon << 1$, in the limit of high energies we have that $\psi_{\mathrm{eq},S11+} > 0$ and $\psi_{\mathrm{eq},S11-} < 0$. Hence, with increasing energy the in-phase motion $S11+$ localizes to the LO, while the out-of-phase motion $S11-$ localizes to the nonlinear attachment (the NES).

Considering now the low-energy limit, it is easily shown that for sufficiently small values of r the equilibrium equation for ψ_{eq} leads to the simple limiting relation $\cos\psi_{\mathrm{eq}} \rightarrow 0$. Therefore, we conclude that as $r \rightarrow 0+$, the following values are attained by the equilibrium value for ψ:

$$\lim_{r\to 0+} \psi_{\mathrm{eq},S11+} = -\pi/2 \text{ and } \lim_{r\to 0+} \psi_{\mathrm{eq},S11-} = +\pi/2$$

It follows that in the limit of small energies the in-phase periodic motion on $S11+$ localizes to the nonlinear oscillator, while the out-of-phase periodic motion on $S11-$ to the LO. However, unlike the high-energy limits (9), as $r \to 0$ localization is *complete* in either the LO or the nonlinear attachment.

In the transition from high to low energies, the out-of-phase $S11-$ undergoes two saddle-node bifurcations. In the first bifurcation, a new pair of stable-unstable equilibrium points is generated near $\psi = +\pi/2$. As energy decreases a second (inverse) saddle-node bifurcation occurs that destroys the unstable equilibrium generated in the first bifurcation together with the branch of $S11-$ that existed for higher energies (Figure 1). It should be noted, however, that these bifurcations occur only below a certain critical mass ratio ε, e.g., only for sufficiently light attachments

2.1 Impulsive Orbits

When the initial energy in the system is localized to the linear oscillator, the transient phase of the response corresponds to a trajectory with initial condition $\psi(0) = \pi/2$. In terms of the spherical topology of phase space this corresponds to a trajectory that initially lies at NP, and is referred to as impulsive orbit (IO).

The IO, computed from the slow flow (7), together with the trajectory passing through the SP (corresponding to the orbit having as only nonzero initial condition the velocity of the LO) are shown in Figure 2 for varying values of the energy-like parameter r (e.g., on different isoenergetic manifolds). We note that the depicted IOs may be either periodic or quasiperiodic. In Figures 2c,d a third isolated trajectory is seen which lies at the same energy level as the trajectory passing through the NP.

Starting from the low-energy isoenergetic manifold of Figure 2a, we note that the IO makes a small excursion in the spherical phase space, and remains localized close to $\psi = +\pi/2$; it follows that in this case, the energy exchange between the LO to the nonlinear attachment is insignificant, and the oscillation remains confined predominantly to the LO. The same qualitative behavior is observed until the critical energy $r = r_{critical} = 0.3865$ (occurring between Figures 2d,e), for which the IO coincides with two homoclinic loops in phase space; these turn out to be the homoclinic loops of the unstable hyperbolic equilibrium on $S11-$ existing between the two saddle-node bifurcations discussed previously. For $r > r_{critical}$ the topology of the IO changes drastically, as it makes much larger excursions in phase space; this means continuous, strong energy exchange between the LO and the nonlinear attachment in the form of a nonlinear beat. At an even higher value of energy, $r \approx 0.4495$, the IO passes through both the NP and SP (this occurs between Figures 2g,h), and

100% of the energy is transferred back and forth between the LO and the nonlinear attachment during the nonlinear beat.

The energy level $r = r_{complete}$ for which complete energy exchange occurs between the LO and the nonlinear attachment during the beating phenomenon is related to the energy of the impulsive orbit and the energy of the trajectory passing through the SP as

$$h_{NP} = \frac{r^2}{2} + \frac{3Cr^4}{32} \quad \text{and} \quad h_{SP} = \frac{r^2}{4} + \frac{3Cr^4}{32\varepsilon^2} \qquad (10)$$

Equating these two energies, we ensure that there is entire energy transfer from the LO to the nonlinear attachment. This provides the value for $r_{complete}$:

$$h_{NP} = h_{SP} \Rightarrow r_{complete} = \left[8\varepsilon^2 \big/ 3C(1-\varepsilon^2)\right]^{1/2} \qquad (11)$$

For $\varepsilon = 0.1$ and $C = 2/15$, we obtain $r_{complete} = 0.4495$, which is in agreement with the results depicted in Figure 2.

It turns out that the critical value of the energy-like variable, $r_{critical}$, can be directly related to the existence of a critical energy level in the underlying Hamiltonian system, above which the IO makes large excursions in phase space and nonlinear beats with strong energy exchanges between the LO and the nonlinear attachment are initiated.

3. Conditions for Optimal Fundamental TET

We reconsider the two-DOF system (1) with $\lambda_1 = \lambda_2 = \varepsilon\lambda$ and $\omega_0^2 = 1$, and initial conditions corresponding to excitation of an impulsive orbit (IO), $v(0) = \dot{v}(0) = x(0) = 0$ and $\dot{x}(0) = X$, and $0 < \varepsilon << 1$. In Figure 3 we depict the dissipation of instantaneous energy in the system with $\varepsilon = 0.05$,

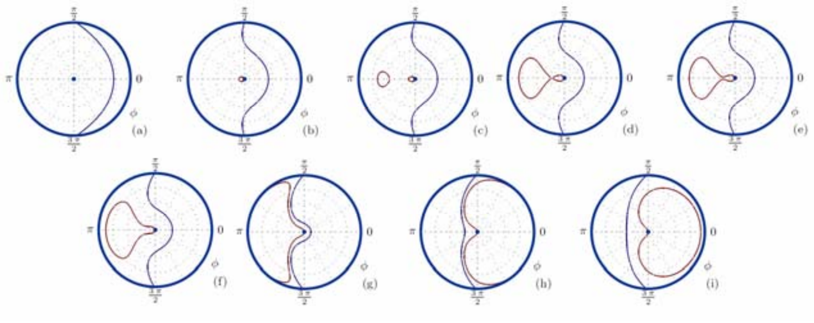

Figure 2: IOs passing through the NP (the origin of the projection), and orbits passing through the SP (ε =0.1, C=2/15): (a) r = 0.25, (b) r = 0.36, (c) r = 0.37, (d) r = 0.386, (e) r = 0.387, (f) r = 0.40, (g) r = 0.44, (h) r = 0.46, (i) r = 0.50; the shift of the IO between Figures 3g,h is an artifact of the projection.

$C = 1$ and $\varepsilon\lambda = 0.005$ (these parameter values will be used in the remainder of this section, unless stated otherwise), when damped IOs are excited. As in the previous section, we find that strong energy dissipation, e.g., strong TET, is realized in the intermediate energy region, in the neighborhood of the 1:1 resonance manifold of the underlying Hamiltonian system.

As shown below, it is the homoclinic orbit of this hyperbolic periodic orbit that affects the topology of nearby IOs and defines conditions for optimal TET in the weakly damped system.

Applying the complexification-averaging method

$$\psi_1(t) = \dot{v}(t) + jv(t) \equiv e^{jt}(u+w)/(1+\varepsilon),$$
$$\psi_2(t) = \dot{x}(t) + jx(t) \equiv e^{jt}(w-\varepsilon u)/(1+\varepsilon) \tag{12}$$

we derive the following set of complex modulation equations after averaging the fast term e^{jt}.

$$\dot{u} + \frac{(1+\varepsilon)\lambda}{2}u - \frac{3(1+\varepsilon)jC}{8\varepsilon}|u|^2 u + j\frac{u+w}{2(1+\varepsilon)} - \varepsilon\lambda\frac{w-\varepsilon u}{2(1+\varepsilon)} = 0$$
$$\dot{w} + j\varepsilon\frac{u+w}{2(1+\varepsilon)} + \varepsilon\lambda\frac{w-\varepsilon u}{2(1+\varepsilon)} = 0 \tag{13}$$

with initial conditions $u(0) = -X$ and $w(0) = X$. Thus we have reduced the problem of studying intermediate-energy damped IOs of the initial system of coupled oscillators (1) to the above system of first order complex modulation equations which govern the slow flow close to the 1:1 resonance manifold. These equations are valid only for small- and moderate-energy IOs, e.g., for initial conditions $X < 0.5$ (cf. Figure 3a), since above this level the fast frequency of the response depends significantly on the energy level and the assumption $\omega \approx 1$ is violated.

Since we are interested in the study of optimal energy dissipation, especially from the NES, we approximate the dissipated energy due to the damper of the NES, as:

$$E_{DISS}(t) = \varepsilon\lambda\int_0^t [\dot{x}(t) - \dot{v}(t)]^2\, dt = \frac{\varepsilon\lambda}{2}\int_0^t |u(t)|^2\, dt$$

where the last equality follows from (12) by omitting terms with fast frequencies greater than unity from the integrand (consistent with the previous averaging). It follows, that enhanced TET in system (1) is associated with the modulus $|u(t)|$ attaining large amplitudes, especially during the initial phase of motion where the energy is at its highest values.

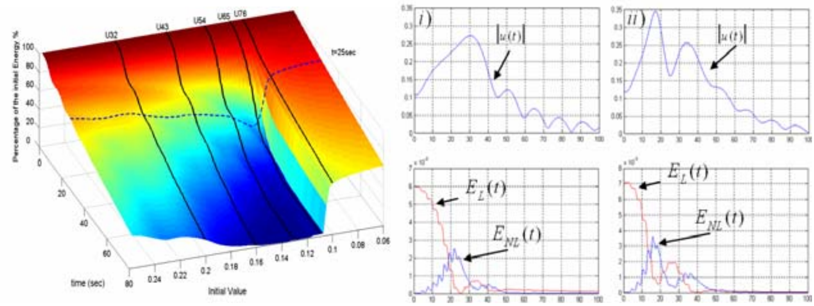

Figure 3. a) Percentage of energy dissipated in system (1) when intermediate-energy damped IOs are excited: solid lines correspond to excitation of specific periodic IOs, and the dashed line indicates the energy remaining in the system at t=25s. b) Slow-flow (13) or (15) of damped IOs in the intermediate-energy regime: (i) X=0.11 (optimal TET) (ii) X=0.12.

Returning to the slow-flow (13), the second modulation equation can be solved explicitly as follows,

$$w(t) = X\, e^{-\frac{\varepsilon(j+\lambda)t}{2}} + \frac{\varepsilon(\varepsilon\lambda - j)}{2(1+\varepsilon)} \int_0^t e^{-\frac{\varepsilon}{2}(j+\lambda)[t-\tau]} u(\tau)\, d\tau \qquad (14)$$

which, upon substitution into the first modulation equation yields:

$$\dot{u} - \frac{3jC(1+\varepsilon)}{8\varepsilon}|u|^2 u + \frac{j+\lambda\left[\varepsilon^2+(1+\varepsilon)^2\right]}{2(1+\varepsilon)} u = \frac{\varepsilon\lambda - j}{2(1+\varepsilon)} X e^{\frac{\varepsilon(j+\lambda)t}{2}} + \varepsilon\left[\frac{(\varepsilon\lambda - j)}{2(1+\varepsilon)}\right]^2 \int_0^t e^{\frac{\varepsilon}{2}(j+\lambda)[t-\tau]} u(\tau)\, d\tau \quad (15)$$

This complex integro-differential equation governs the slow-flow of a damped IO in the intermediate-energy regime, as it is equivalent to system (13). The above dynamical provides information on the slow evolution of the damped dynamics close to the 1:1 resonance manifold.

In Figure 3b we show the dynamics of the averaged system (13) [or equivalently (15)] for two initial values close to the homoclinic orbit. As we are able to observe, in Figure 3b(i) we have a slow oscillation during which the entire energy of the LO gets transferred to the NES over a single half-cycle.

Hence, we consider the modulation equation (15) and restrict the analysis to the initial stage of the dynamics. Mathematically, we will be interested in the dynamics up to times of $O(1/\varepsilon^{1/2})$, for initial conditions (impulses) or order $X = O\left(\varepsilon^{1/2}\right)$. Under these assumptions the integral term on the right-hand-side of (15) is expressed as follows:

$$I = \varepsilon\left[2(1+\varepsilon)\right]^{-2} \int_0^t e^{-\frac{\varepsilon}{2}(j+\lambda)[t-\tau]} u(\tau)\, d\tau + O\left(\varepsilon^2\right)$$

When $t = O\left(\varepsilon^{-1/2}\right)$, we have also that $\left|\tau - t\right| = O\left(\varepsilon^{-1/2}\right)$; it follows that by expanding the exponential in the integrand in Taylor series in terms of ε and using the mean value Theorem of integral calculus, the integral is ordered as, $I = O\left(\varepsilon\right)$, and hence is a small quantity.

Taking this result into account, and introducing the variable transformations, $u = \left(4\varepsilon/3C\right)^{1/2} z$, $B = -\left(3C/4\varepsilon\right)^{1/2} X$ to account for the scaling of the initial condition (impulse) $X = O\left(\varepsilon^{1/2}\right)$ and $\lambda = \varepsilon^{1/2}\hat{\lambda}$ for the damping coefficient, we express the modulation equation (15) in the form,

$$\dot{z} - \frac{j}{2}\left|z\right|^2 z + \frac{j + \varepsilon^{1/2}\hat{\lambda}}{2} z = \frac{jB}{2} + O(\varepsilon),\ z(0) = B, \quad (16)$$

and all quantities other than the small parameter ε are assumed to be $O(1)$ quantities. The complex modulation equation (16) provides an approximation to the initial slow-flow dynamics, and is valid formally up to times of $O\left(\varepsilon^{-1/2}\right)$.

Introducing the polar transformation, $z = Ne^{j\delta}$, substituting into (16), and separating real and imaginary parts this system can be expressed as,

$$\begin{aligned} &\dot{N} + \frac{\varepsilon^{1/2}\hat{\lambda}}{2} N = \frac{B}{2}\sin\delta + O(\varepsilon), \qquad N(0) = B \\ &\dot{\delta} + \frac{1}{2} - \frac{1}{2}N^2 = \frac{B}{2N}\cos\delta + O(\varepsilon), \quad \delta(0) = 0 \end{aligned} \quad (17)$$

Reconsidering the system (16-17), we seek its solution in the following regular perturbation form:

$$z(t) = z_0(t) + \varepsilon^{1/2}\hat{\lambda}\, z_1(t) + O\left(\varepsilon\right),\ \text{and}\ B = B_0 + \varepsilon^{1/2}\hat{\lambda} B_1 + O\left(\varepsilon\right) \quad (18)$$

Substituting into (16) and considering only $O(1)$ terms we derive the following system:

$$\dot{z}_0 - \frac{j}{2}\left|z_0\right|^2 z_0 + \frac{j}{2} z_0 = \frac{jB_0}{2},\quad z_0(0) = B_0 \qquad (19a)$$

or, in terms of the transformation $z_0 = N_0 e^{j\delta_0}$,

$$\dot{N}_0 = \frac{B_0}{2}\sin\delta_0,\quad N_0(0) = B_0\ \text{ and }\ \dot{\delta}_0 + \frac{1}{2} - \frac{1}{2}N_0^2 = \frac{B_0}{2N_0}\cos\delta_0,\quad \delta_0(0) = 0 \quad (19b)$$

We note that damping effects enter into the problem at the problem of the next order of approximation.

It can be proved that the undamped slow-flow possess the following Hamiltonian

$$\frac{j}{2}|z_0|^2 - \frac{j}{4}|z_0|^4 - \frac{jB_0}{2} z_0^* - \frac{jB_0}{2} z_0 = h \qquad (20)$$

where the asterisk denotes complex conjugate, which reduces (19b) to the following one-dimensional slow-flow,

$$2\dot{a} = \left[4B_0 a - \left(a - \frac{1}{2}a^2 + \frac{1}{2}B_0^4 + B_0^2 \right)^2 \right]^{1/2}$$
$$\sin\delta_0 = \frac{2}{B_0}\frac{d\sqrt{a}}{dt}, \quad a(0) = B_0^2, \quad \delta_0(0) = 0 \qquad (21)$$

where we introduced the notation $a(t) \equiv N_0^2(t)$. The roots of the r.h.s. depend on the parameter B_0. For $B_0 > B_{0cr} \approx 0.36727$ the r.h.s. possesses two real distinct roots for a, whereas for $B_0 < B_{0cr}$ four distinct real roots. For $B_0 = B_{0cr}$ two of the real roots coincide, so the r.h.s possesses only three distinct real roots. In this case, it will be proven that the system (21) possesses a homoclinic orbit, which we now proceed to compute explicitly.

Indeed, for $B_0 = B_{0cr}$ the reduced slow-flow dynamical system can be integrated by quadratures as to yield the following analytical homoclinic orbit of the first-order system (19),

$$a_h(t) = a_2 - \frac{\gamma_1\gamma_2}{\gamma_1 \sinh^2\left(\frac{\sqrt{\gamma_1\gamma_2}}{8}t\right) + \gamma_2\cosh^2\left(\frac{\sqrt{\gamma_1\gamma_2}}{8}t\right)} \quad and \quad \delta_0(t) = \delta_{0h}(t) = \sin^{-1}\left[\frac{2}{B_{0cr}}\frac{d\sqrt{a_h^{(-)}(t)}}{dt}\right] \qquad (22)$$

where, $\gamma_1 = a_2 - B_{0cr}^2$, $\gamma_2 = a_4 - a_2$, and only the branch of the solution corresponding to $t \geq 0$ is taken. The solution (22) assumes the limiting values, $N_0(0) = B_{0cr}$ and $\lim_{t\to+\infty} N_0(t) = \sqrt{a_2}$. Of course, the solution (22) can be extended for $t < 0$, but the resulting branch of the homoclinic orbit is not a solution of the problem (19a). We mention that the system (21) provides an additional homoclinic loop which however does not satisfy the initial condition.

This completes the solution of the O(1) approximation of the homoclinic solution of (16-17), and we now consider the $O(\varepsilon)$ problem, which takes into account (to the first order) the effects of damping. We will be especially interested to study the perturbation of the homoclinic solution of the $O(1)$ problem when weak damping [of $O(\varepsilon^{1/2})$] is added. The $O(\varepsilon^{1/2})$ analysis will also provide a correction due to damping of the critical value of the impulse (initial condition) corresponding to the homoclinic solution.

Substituting (18) in (16) and considering $O(\varepsilon^{1/2})$ terms, we derive the following problem at the next order of approximation:

$$\dot{z}_1 - \frac{j}{2}\left(z_1^* z_0^2 + 2|z_0|^2 z_1\right) + \frac{j}{2} z_1 = -\frac{1}{2} z_0 + \frac{jB_1}{2},\ \ z_1(0) = B_1$$

This is a complex quasi-linear ordinary differential equation with a nonhomogeneous term. Key in solving the problem, is the computation of two linearly independent homogeneous solutions, since then, a particular integral may be systematically computed by the employing the method of variation of parameters.

By direct substitution into the complex homogeneous equation we can prove that one homogeneous solution that satisfies the initial condition can be computed in terms of the homoclinic solution as, $z_{HS}^{(1)}(t) = x_{HS}^{(1)}(t) + jy_{HS}^{(1)}(t) = 2\dot{z}_{0h}(t) / B_{0cr}$. In addition, the homogeneous solution $z_{HS}^{(1)}(t)$ satisfies the limiting conditions $\lim_{t\to+\infty} x_{1HS}^{(1)}(t) = 0$ and $\lim_{t\to+\infty} y_{1HS}^{(1)}(t) = 0$.

The second linearly independent homogeneous solution is computed by exploiting the Wronskian relation

$$\dot{W}(t) = 0 \Rightarrow x_{1HS}^{(1)}(t) y_{1HS}^{(2)}(t) - x_{1HS}^{(2)}(t) y_{1HS}^{(1)}(t) = 1$$

In this way we finally obtain the solution

$$x_{1HS}^{(2)}(t) = \frac{x_{1HS}^{(1)}(t) y_{1HS}^{(2)}(t) - 1}{y_{1HS}^{(1)}(t)} \text{ and } y_{1HS}^{(2)}(t) = \int_0^t \frac{a_{21}(\tau)}{y_{1HS}^{(1)}(\tau)} \exp\left\{-\int_\tau^t \left[a_{21}(s)\frac{x_{1HS}^{(1)}(s)}{y_{1HS}^{(1)}(s)} + a_{22}(s)\right] ds\right\} d\tau$$

Using the fundamental solution we obtain the $O(\varepsilon^{1/2})$ perturbation of the homoclinic orbit:

$$\begin{Bmatrix} x_{1h}(t) \\ y_{1h}(t) \end{Bmatrix} = \begin{Bmatrix} x_{1HS}^{(2)}(t) \\ y_{1HS}^{(2)}(t) \end{Bmatrix} \left[\int_0^t \frac{x_{0h}(\tau)}{2} y_{1HS}^{(1)}(\tau) + \left[\frac{B_{cr} - y_{0h}(\tau)}{2}\right] x_{1HS}^{(1)}(\tau) d\tau - B_{cr}\right] - \begin{Bmatrix} x_{1HS}^{(1)}(t) \\ y_{1HS}^{(1)}(t) \end{Bmatrix} \int_0^t \left\{\frac{x_{0h}(\tau)}{2} y_{1HS}^{(2)}(\tau) + \left[\frac{B_{cr} - y_{0h}(\tau)}{2}\right] x_{1HS}^{(2)}(\tau)\right\} d\tau$$

Then, taking into account that the components of the second homogeneous solution $x_{1HS}^{(2)}(t)$ and $y_{1HS}^{(2)}(t)$ in the second additive term diverge as $t \to +\infty$, in order to get bounded solutions we need

$$B_{1cr} = \int_0^{+\infty} \left[x_{0h}(\tau) y_{1HS}^{(1)}(\tau) - y_{0h}(\tau) x_{1HS}^{(1)}(\tau)\right] d\tau \Bigg/ 2 - \int_0^{+\infty} x_{1HS}^{(1)}(\tau)\, d\tau$$

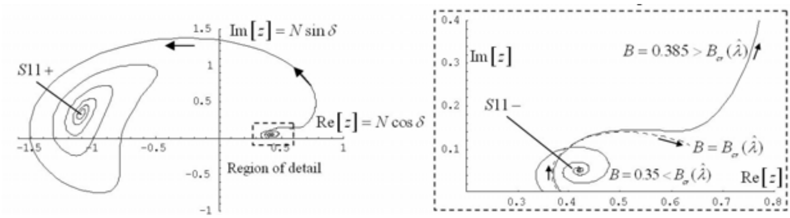

Figure 4. Parametric plots for $\hat{\lambda} = 0.4472$ of Im[z] against Re[z] with t being the parametrizing variable: initial regime of slow-flow dynamics of intermediate-energy damped IOs for different normalized impulses B [slow-flow (16) or (17)].

This completes the solution and proves the perturbation of the homoclinic orbit in the damped system (16-17) with $O(\varepsilon^{1/2})$ damping. For $\varepsilon = 0.05$ and $\hat{\lambda} = 0.4472$ we estimate the initial condition as, $B_{cr} \approx 0.3806$ $\left(X = 0.0983\right)$, which compares to the numerical value of 0.3814 $\left(X = 0.1099\right)$ derived from the numerical integration of the slow-flow (15)(error is of $O(\varepsilon = 0.05)$).

4 Conclusions

The findings of this work confirm that, for sufficiently weak damping, damped transitions are essentially influenced by the underlying Hamiltonian dynamics. A detailed computational study reveals the different types of nonlinear transitions that occur in the weakly damped system. Based on these studies, direct analytical treatment of the governing strongly nonlinear damped equations of motion is performed through slow/fast partition of the transient responses. In this way we determine the characteristic time scales of the dynamics that influence the capacity of the nonlinear attachment to passively absorb and locally dissipate broadband energy from the LO.

References

Arnold, V. I., Kozlov, V. V., Neishtadt, A. I. (1985).*Mathematical Aspects of Classical and Celestial Mechanics*. Springer-Verlag, Berlin.

Kerschen, G., Lee, Y., Vakakis, A., McFarland, M., Bergman, L., (2006) *Irreversible passive energy transfer in coupled oscillators with essential nonlinearity*, SIAM J. Appl. Math., **66**, (648).

Quinn, D., Gendelman, O., Kerschen, G., Sapsis, T., Bergman, L., Vakakis, A., (2007) *Efficiency of targeted energy transfers in coupled nonlinear oscillators associated with 1:1 resonance captures: Part I*, J. Sound Vib., in press.

Sapsis T., Vakakis A., Gendelman, O., Bergman, L., Kerschen, G., Quinn D., (2008) *Efficiency of targeted energy transfers in coupled nonlinear oscillators associated with 1:1 resonance captures: Part II,* , J. Sound Vib., under review.